BULLETIN OF THE POLISH ACADEMY OF SCIENCES
TECHNICAL SCIENCES, Vol. 67, No. 6, 2019
DOI: 10.24425/bpasts.2019.130885



# Input-output decoupling for a 3D free-floating satellite with a 3R manipulator with state and input disturbances

W. DOMSKI* and A. MAZUR

Wrocław University of Science and Technology, Wrocław, Poland

**Abstract.** This work presents the results acquired during simulation studies done for a 3D free-floating satellite behaviour with input-output decoupling approach. The research object is a free-floating satellite with a 3 DoF rigid 3D manipulator where a noise disturbance was introduced. Different approaches are used to compensate the noise influence. Systems using a visual aid to determine the position of manipulator joints are not ideal and introduce some uncertainties. What is more, determining the position from joints encoders is not error-free while computing angular velocity from numerical differentiation introduces even greater disturbance to the system. A couple of scenarios were investigated where state of the manipulator, including its position and velocity, was disturbed with homogeneous noise. Also the control inputs of the manipulator were disturbed. Simulation results show that the biggest impact on the control quality has a scenario where the satellite's state has been disturbed with additive noise.

**Key words:** 3D free-floating satellite, input–output decoupling, control, homogeneous noise.

## 1. Introduction

Space robotics is a continuously developing field where there are many open problems waiting to be solved. One example of such a problem is the task of trajectory planning [16]. Also a satellite with a manipulation arm can be used to remove space rubbish, debris, etc. that are often an unwanted result of space exploration [5, 8, 9]. After successful space missions as well as unsuccessful ones debris which comes from satellites' crash are orbiting Earth. An another source of such objects can be a collision (direct impact of two or more different types of objects) which eventually causes debris floating around the planet to increase. It is a significant problem which unattended, in a near future, can be a serious issue for space craft launching.

The main focus of this work was put on the last stage – the trajectory of space debris which are in close distance to a satellite. While being in a close distance to the object it is possible to track the desired trajectory only by controlling the manipulator arm. Even though, the feedback forces cause the satellite to change its position and orientation but the position of system's mass center is constant. The manoeuvre of intercepting a space object is a not a trivial task mainly due to forces which are present between the chaser and the object itself [1, 3]. Also, some work was done to validate the strategy of approaching and grasping a space object [19]. An another aspect is to ensure that the generated trajectory would be recreated [17, 18]. Moreover, during a manoeuvre of intercepting a target a necessity of avoiding obstacles can arise [15] where the most important task is to avoid debris or different material which could destroy the satellite.

During capturing the object it is necessary to estimate its position. Without a good estimation it is impossible to catch the debris. Those aspects were mentioned in [12] where a method of a perspective circle and line was used to gather the knowledge of a point of interest. Also authors emphasise that the calibration of the camera is crucial due to disturbance it introduces when it is not calibrated. In [23] authors focus on a vision system where they propose a solution for a visual-tracking problem for a free-floating space manipulator. This technique allows also to estimate the uncertainties of object's dynamics.

Moreover, control of a space manipulator is a separate subject which is supported by a great many publications in this area. However, a novel approach to control a space manipulator in case of a single joint failure was presented in [4] where factitious force method was exploited [10].

It is worth mentioning that in the near distance to the object of interest the manipulator workspace is limited and there was a lot of research done on this aspect along with the manipulability of a space manipulator [22].

The research object in this paper is a satellite with a 3 DoF rigid manipulator arm. Considering the nature of the controlled object an input–output decoupling method was used to linearise the model [11]. Thanks to the procedure of linearisation we can control manipulator joints while tracking desired trajectory in external coordinates. The dynamics of examined model was derived from generalized coordinates and the model lives in a 3D space.

Furthermore, one other aspect of a space object control was investigated. The noise disturbance is an accompanying phenomenon during a satellite movement and it can not be completely avoided, only its influence can be diminished. In this work, a number of scenarios were closely examined. During the

*e-mail: wojciech.domski@pwr.edu.pl

Manuscript submitted 2019-01-06, revised 2019-04-02 and 2019-06-03, initially accepted for publication 2019-06-06, published in December 2019

simulation studies four classes of additive disturbances were taken into account. The first class is an ideal case where there is no noise. The second class is when some noise is present but applies to the state vector considering only the manipulator joints and its velocities. The next class was disturbance impact on control signals while the last class was a mixture of the last two.

In the Section 2 kinematics of the space manipulator was presented while the Section 3 contains some information on the model's state vector and describes dynamics of our system while Section 4 states the control problem. The input-output decoupling procedure was discussed in the Section 5. The problem of noise disturbance along with different scenarios was described in the Section 6. Simulation results were collected and presented in the Section 7. The discussion of results and summary was included in the Conclusions.

## 2. Satellite kinematics

The satellite's base is a cuboid. A rigid 3R manipulator is mounted on the satellite's base which can track a trajectory in the 3D space associated with the global coordination system $X_0Y_0Z_0$. Placement of a local coordination system $X_bY_bZ_b$ is associated with the satellite's mass center. It can be presented as the following relation

$$A_0^b(q_b) = Trans(X, x)\,Trans(Y, y)\,Trans(Z, z)\cdot \cdot Rot(X, \alpha)\,Rot(Y, \beta)\,Rot(Z, \gamma). \tag{1}$$

The Euler angles were selected as $XYZ(\phi, \theta, \psi)$ where $\alpha = \phi$, $\beta = \theta$ and $\gamma = \psi$. Furthermore, the limitations of Euler angles are described as $0 < \phi < 2\pi$, $0 < \theta < \pi$ and $0 < \psi < 2\pi$. Placement of the end of manipulator's first link in relation to global coordination system $X_0Y_0Z_0$ is defined as the following transformation

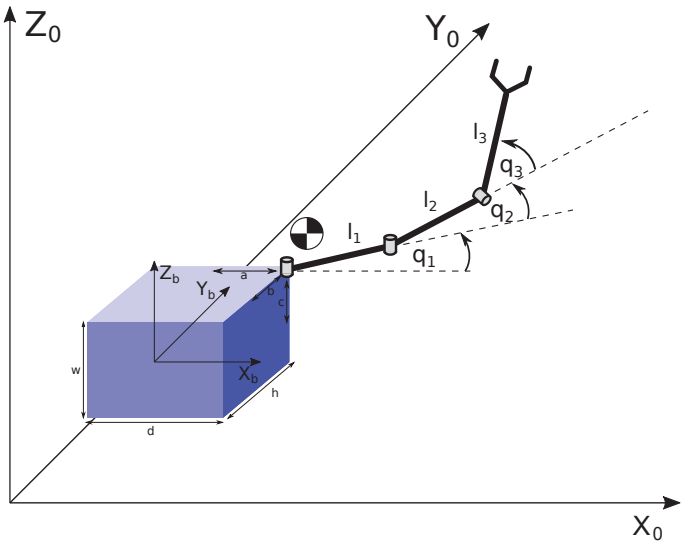


Fig. 1. Satellite's model with marked coordination systems

$$A_0^1(q_b, q_r) = A_0^b Trans(X, a)\,Trans(Y, b)\,Trans(Z, c)\cdot \cdot Rot(Z, q_1)\,Trans(X, l_1). \tag{2}$$

The position of the end of the second link is described as

$$A_0^2(q_b, q_r) = A_0^1 Rot(Z, q_2)\,Trans(X, l_2)\,Rot\left(X, \frac{\pi}{2}\right). \tag{3}$$

Lastly, the position of the third link, the end effector, is presented in the following relation

$$A_0^3(q_b, q_r) = A_0^2 Rot(Z, q_3)\,Trans(X, l_3). \tag{4}$$

The $A_0^3(q_b, q_r)$ can be used to derive the end-effector position, thus its kinematic can be described as

$$y = \begin{pmatrix} x_{eff} \\ y_{eff} \\ z_{eff} \end{pmatrix} = k(q_b, q_r). \tag{5}$$

The position vector has a following form

$$q = \begin{pmatrix} q_b \\ q_r \end{pmatrix}, \tag{6}$$

where $q_b = (x, y, z, \alpha, \beta, \gamma)^T$ and $q_r = (q_1, q_2, q_3)^T$. The respective velocities are denoted as

$$\dot{q} = \begin{pmatrix} \dot{q}_b \\ \dot{q}_r \end{pmatrix} \in R^9. \tag{7}$$

$q_b \in R^6$ and $q_r \in R^3$. What is more, $q_b$ consists of 3 elements related to the satellite position in $R^3$ and 3 Euler angles. $SO(3)$ group is a matrix which contains 9 elements but has 6 constraints. The matrix can be expressed as

$$R = \begin{bmatrix} r_1 & r_2 & r_3 \end{bmatrix} \tag{8}$$

where $r_i$ is a column belonging to $R^3$ of the rotation matrix. As mentioned earlier, there are 6 constraints:

$$\|r_1\| = \|r_2\| = \|r_3\| = 1, \tag{9}$$

$$r_1 \times r_2 = r_3, \tag{10}$$

$$r_2 \times r_3 = r_1, \tag{11}$$

$$r_3 \times r_1 = r_2. \tag{12}$$

Therefore, if there are 6 constraints there are 3 angles which parametrize the rotation matrix. What is more, this is the reason for angles belonging to $R^3$.

## 3. Mathematical model of 3D free-floating satellite

The dynamics of the 3D free-floating satellite was expressed in generalized coordinates where the vector describing position has 9 elements and can be divided into two parts. First part is related to the satellite's base position and orientation, while the second part describes the manipulator joint positions. The state vector of the satellite with a 3R manipulator consists of its position and their time derivatives.

**3.1. Pseudoinertia matrices.** For further consideration it was assumed that the three links of the manipulator are rods with uniformly distributed mass. The mass of each rod is $m_i$ while $l_i$ is the length of $i$-th link. Following this assumption the pseudoinertia matrix of a single manipulator's link has a following form

$$J_i = \begin{bmatrix} \frac{1}{3}m_i l_i^2 & 0 & 0 & -\frac{1}{2}m_i l_i \\ 0 & 0 & 0 & 0 \\ 0 & 0 & 0 & 0 \\ -\frac{1}{2}m_i l_i & 0 & 0 & m_i \end{bmatrix}, \quad i = 1, 2, 3. \tag{13}$$

Lower index $i = 1, 2, 3$ determines the link number.

The satellite base has a mass $m_b$ and is modelled as a cuboid with width $w$ (along local $Y$ axis), height $h$ (along local $Z$ axis) and depth $d$ (along local $X$ axis). For such a 3D object the pseudoinertia matrix has following form

$$J_b = \begin{bmatrix} \frac{1}{12}m_b d^2 & 0 & 0 & 0 \\ 0 & \frac{1}{12}m_b w^2 & 0 & 0 \\ 0 & 0 & \frac{1}{12}m_b h^2 & 0 \\ 0 & 0 & 0 & m_b \end{bmatrix}. \tag{14}$$

**3.2. Total kinetic energy.** The base kinetic energy can be calculated in the following manner

$$E_b = \frac{1}{2}\, tr\left\{\dot{A}_0^b J_b \left(\dot{A}_0^b\right)^T\right\} = \frac{1}{2}\dot{q}^T Q_b \dot{q}. \tag{15}$$

The kinetic energy of an $i$-th link can be derived from the similar formula given below as

$$E_i = \frac{1}{2}\, tr\left\{\dot{A}_0^i J_i \left(\dot{A}_0^i\right)^T\right\} = \frac{1}{2}\dot{q}^T Q_i \dot{q}. \tag{16}$$

**3.4. Inertia matrix.** The inertia matrix of the whole system consisting of a cuboid base and a manipulator with 3 DoF can be expressed as a sum of inertia matrices of each term ($Q_b$, $Q_1$, $Q_2$ and $Q_3$).

$$M = Q_b + \sum_{i=1}^{3} Q_i. \tag{17}$$

**3.4. Coriolis and centrifugal forces matrix.** The Coriolis matrix can be calculated from the inertia matrix $M$ by using the Christoffel symbols of the first kind. $C \in R^{9\times 9}$ and each term is equal to

$$C_{ij}(q, \dot{q}) = \sum_{k=1}^{n} c_{kj}^i(q)\dot{q}_k, \tag{18}$$

where

$$c_{kj}^i(q) = \frac{1}{2}\left(\frac{\partial M_{ij}}{\partial q_k} + \frac{\partial M_{ik}}{\partial q_j} - \frac{\partial M_{jk}}{\partial q_i}\right). \tag{19}$$

**3.5. Dynamics in barycentric coordinates.** A rigid manipulator with a free-floating base can be described using following dynamics [20]

$$M\ddot{\hat{q}} + C\dot{\hat{q}} = \begin{pmatrix} 0 \\ u \end{pmatrix}, \tag{20}$$

or more in detail as

$$\begin{bmatrix} M_b & M_{bm} \\ M_{bm}^T & M_m \end{bmatrix}\begin{pmatrix} \ddot{\hat{q}}_b \\ \ddot{q}_r \end{pmatrix} + \begin{pmatrix} c_b \\ c_r \end{pmatrix} = \begin{pmatrix} 0 \\ u \end{pmatrix} \tag{21}$$

where $M$ is an inertia matrix of the whole system including the satellite base and the 3R manipulator. Additional elements of the dynamics such as Coriolis and centrifugal forces were includes within terms described as $c_b$ and $c_r$. The $u$ is a torque input control vector of manipulator joints. Vector $\hat{q}$ is similar to vector $q$ but instead of satellite position, the first 3 elements contain the position of the center of the mass of the whole system – the satellite and the manipulator.

$$\hat{q} = \begin{bmatrix} \hat{x} & \hat{y} & \hat{z} & \alpha & \beta & \gamma & q_1 & q_2 & q_3 \end{bmatrix}^T. \tag{22}$$

Therefore, the model is expressed in barycentric coordinates instead of generalized coordinates. Using barycentric coordinate system allows to maintain the constant momentum of the system (momentum conservation) [13].

During the model calculation it was assumed that the system is in the space, therefore in the environment where gravity can be omitted. The satellite's base is a free-floating satellite which means that its mass center position can not be directly influenced. Those assumptions were incorporated into the dynamics model.

We can define dynamics of our system in respect to the satellite [20] as

$$M_b\ddot{\hat{q}}_b + M_{bm}\ddot{q}_r + c_b = J_b^T F_h \tag{23}$$

where $F_h$ is a vector of external forces exerted on the system. Since there are no external forces, $F_h = 0$ and $c_b$ is defined as

$$c_b = \dot{M}_b\dot{\hat{q}}_b + \dot{M}_{bm}\dot{q}_r, \tag{24}$$

the first row of dynamics equations (21) can be rewritten as

$$M_b\ddot{\hat{q}}_b + M_{bm}\ddot{q}_r + c_b = 0. \tag{25}$$

Putting $c_b$ into above equation we can observe that

$$\frac{d}{dt}\left(M_b\dot{\tilde{q}}_b + M_{bm}\dot{q}_r\right) = M_b\ddot{\tilde{q}}_b + M_{bm}\ddot{q}_r + c_b = 0. \quad (26)$$

thus

$$M_b\dot{\tilde{q}}_b + M_{bm}\dot{q}_r = const. \quad (27)$$

## 4. Control problem statement

Let's consider a free-floating satellite which is a not propelled space object with a 3 DoF rigid manipulator attached to its base. Because the satellite has no thrusters we can not directly influence the position and the orientation of the satellite's base in space. We also assume the following:

**Assumption 1.** The system has a constant momentum which means that the satellite moves with constant velocity. Moreover, the corresponding coordinate system attached to the mass center of the whole system does not move in relation to the chased object.

The task is to follow a desired trajectory which can mimic the chase after a space object, i.e. debris. The system consisting of a satellite and a chased object does not have to be in rest. In other words, it is only required that the satellite's mass center does not move in relation to chased object's mass center.

The satellite's task is to move the end-effector along a $C^2$ trajectory which is inside the operating space of the arm. This task can be also considered as an obstacle avoidance in the near of a satellite or a first stage of capturing the object.

Moreover, the satellite is not equipped with reaction wheels or thrusters which could change the momentum of the object.

**Assumption 2.** To fulfil such a task we have proposed a control algorithm which uses the input-output decoupling method for an object with fully known dynamics. In this work we consider a case where the satellite is treated as an under-actuated system (21).

## 5. Input-output decoupling control

The satellite has no thrusters, thus its position and orientation cannot be directly influenced. A model of a satellite in generalized coordinates was presented in this work. For the dynamics described by (21) we have relation between control input and its state.

The input-output decoupling algorithm is a description of a model where the relation between the input to the state of the system (the dynamics) and the relation between the state to the output (the kinematics) is exploited. Let

$$y_i = k_i(q), \quad i = 1, \ldots, m, \quad (28)$$

where $k_i\ (q)$ is an $i$-th element of the end-effector kinematics. Then

$$\dot{y}_i = \frac{d}{dt}k_i(q) = \frac{\partial k_i}{\partial q}\frac{dq}{dt} = J_i(q)\dot{q}. \quad (29)$$

The time derivative of above equation yields

$$\begin{aligned}\ddot{y}_i &= \frac{d^2}{dt^2}k_i(q) = \dot{J}_i(q)\dot{q} + J_i(q)\ddot{q} = \\ &= \dot{q}^T\frac{\partial^2 k_i}{\partial q^2}\dot{q} + J_i\ddot{q} = P_i + J_i\ddot{q}.\end{aligned} \quad (30)$$

Collecting all output variables a matrix equation can be obtained

$$\ddot{y} = P + J\ddot{q}. \quad (31)$$

Let the dynamic equation of a manipulator mounted on a satellite be given as

$$M\ddot{q} + C\dot{q} = \begin{pmatrix}0\\ u\end{pmatrix}. \quad (32)$$

The real inertia matrix $M$ is always non-singular, therefore we can reformulate (32) to

$$\ddot{q} = M^{-1}\left[\begin{pmatrix}0\\ u\end{pmatrix} - C\dot{q}\right]. \quad (33)$$

After substitution of dynamic equation (33) to (31) it yields

$$\begin{aligned}\ddot{y} &= P + JM^{-1}\left[\begin{pmatrix}0\\ u\end{pmatrix} - C\dot{q}\right] = \\ &= P - JM^{-1}C\dot{q} + JM^{-1}\begin{pmatrix}0\\ u\end{pmatrix}.\end{aligned} \quad (34)$$

The equation (34) is an affine system

$$\ddot{y} = F + G\begin{pmatrix}0\\ u\end{pmatrix} \quad (35)$$

where $F = P - JM^{-1}C\dot{q}$ and $G = JM^{-1}$. Furthermore, the $G$ matrix size is important and the matrix itself is not square and can not be directly inverted. However, a part of (35) that describes the control can be reformulated into

$$G\begin{pmatrix}0\\ u\end{pmatrix} = \begin{bmatrix}G_0 & \bar{G}\end{bmatrix}\begin{pmatrix}0\\ u\end{pmatrix} = \bar{G}u, \quad (36)$$

where $\bar{G}$ matrix is square and invertible and its dimension is $m \times m$.

Putting the control law given below as

$$u = \bar{G}^{-1}(-F + v) \tag{37}$$

to the affine system (35), where $v$ is a new input to the system, we obtain a closed-loop system expressed in the form of a double linear integrator.

$$\ddot{y} = v. \tag{38}$$

To ensure that the end-effector will follow a desired trajectory by moving only its joints we propose a PD controller with correction

$$v = \ddot{y}_d - K_d\dot{e} - K_p e, \tag{39}$$

where $y_d$ is a desired trajectory of the end-effector, $K_p = K_p^T > 0$, $K_d = K_d^T > 0$, and the system error is defined as $e = y - y_d$ and its time derivative equals to $\dot{e} = \dot{y} - \dot{y}_d$. To ensure that the procedure of the input-output decoupling is possible to derive, the necessary condition defined by Isidori in [6] has to be met. It says that the number of inputs to the system has to be equal to the number of system's outputs.

## 6. Noise disturbance

Estimating the position and the velocity of manipulator joints is a challenging task. Before implementing the real controller it is necessary to check how well the proposed algorithm is performing when noise is present, as it is in real-life applications. Therefore, a considered model of a free-floating satellite was extended with additional noise variables to resemble the real object. Following equation describes a model where disturbance to the state variables of a manipulator was added. What is more, noise added to the control signals was also taken into account.

$$M(\bar{q})\ddot{q} + C(\bar{q}, \dot{\bar{q}})\dot{\bar{q}} = \begin{pmatrix} 0 \\ \bar{u} \end{pmatrix} \tag{40}$$

where $\bar{q} = [q_b, \bar{q}_r]^T$ and $\dot{\bar{q}} = [\dot{q}_b, \dot{\bar{q}}_r]^T$.

- **Disturbed state signal:** state variable defining manipulator joints is defined as

$$\bar{q}_r = q_r + \delta_0,$$

where $\delta_0$ is a vector of random noise.

- **Disturbed velocity signal:** similarly, the first derivative of manipulator joints' angles is defined as

$$\dot{\bar{q}}_r = \dot{q}_r + \delta_1$$

where $\delta_1$ is a second random noise vector.

- **Disturbed input:** the control signal vector with some noise

$$\bar{u} = u + \delta_u.$$

As it was discussed before the noise disturbance is an accompanying phenomenon during satellite control due to presence of noise in measurements. In this work four classes of noise disturbance and nine scenarios in total were examined. The first class is an ideal case where there is no noise. The simulation results for this scenario were used as a reference point. The second class concerns a situation when some noise is present but it is applied only to the state vector considering the manipulator joints and its velocities. This is common due to measurements of joint position and velocity. The position of a rotary joint can be measured accurately but only to some degree while the measurement of the angular velocity of manipulator joint is challenging [14]. The other class was disturbance noise added only to control signals. Calculating control signals based on the model is an ideal case, however, execution of calculated control signals can have a negative and unwanted effects on the control quality. The last class is a mixture of the last two classes where both noise in state vector and in the input signals is present.

In the Table 1 noise parameters for each scenario were collected. The scenario number 0 is a case where no noise was introduced to the system, thus it is an ideal case, a reference point. All scenarios beside the one described above were simulated with additive noise where disturbance was of a homogeneous nature with limits given in Table 1.

Table 1
Range of $\delta_0$, $\delta_1$ and $\delta_u$ disturbance for each scenario

| Scenario number | $\delta_0$ | $\delta_1$ | $\delta_u$ |
|---|---|---|---|
| 0 | 0 | 0 | 0 |
| 1 | $[-10^{-4}; 10^{-4}]$ | $[-10^{-5}; 10^{-5}]$ | 0 |
| 2 | $[-10^{-4}; 10^{-4}]$ | $[-10^{-5}; 10^{-5}]$ | $[-10^{-3}; 10^{-3}]$ |
| 3 | $[-10^{-4}; 10^{-4}]$ | $[-10^{-5}; 10^{-5}]$ | $[-10^{-2}; 10^{-2}]$ |
| 4 | $[-10^{-2}; 10^{-2}]$ | $[-10^{-3}; 10^{-3}]$ | 0 |
| 5 | $[-10^{-2}; 10^{-2}]$ | $[-10^{-3}; 10^{-3}]$ | $[-10^{-3}; 10^{-3}]$ |
| 6 | $[-10^{-2}; 10^{-2}]$ | $[-10^{-3}; 10^{-3}]$ | $[-10^{-2}; 10^{-2}]$ |
| 7 | 0 | 0 | $[-10^{-3}; 10^{-3}]$ |
| 8 | 0 | 0 | $[-10^{-2}; 10^{-2}]$ |

## 7. Simulations

Simulation studies were conducted for the trajectory tracking problem of a free-floating satellite. The desired trajectory of the end-effector was following

$$\begin{aligned} x_{ef} &= r \cdot \cos(\omega t) + d_x, \\ y_{ef} &= r \cdot \sin(\omega t) + d_y, \\ z_{ef} &= 0 \end{aligned}$$

where $r = 0.5$ [m], $\omega = 0.03\pi$, $d_x = 2.3$ [m] and $d_y = 0.1$ [m]. The gain coefficients of dynamic controller were $K_p = 10$ and $K_d = 50$.

Mass and geometric properties of the satellite and its manipulator were presented below in Table 2.

Table 2
Mass and geometric properties of the satellite

| Symbol | Value | Description |
|---|---|---|
| $w$ | 0.5 [m] | satellite's width |
| $h$ | 0.5 [m] | satellite's height |
| $d$ | 0.5 [m] | satellite's depth |
| $a$ | 0.2 [m] | manipulator displacement along $X_b$ |
| $b$ | 0.2 [m] | manipulator displacement along $Y_b$ |
| $c$ | 0.25 [m] | manipulator displacement along $Z_b$ |
| $m_i$ | 1 [kg] | mass of i$^{th}$ link |
| $l_i$ | 1 [m] | length of i$^{th}$ link |
| $m_b$ | 35 [kg] | mass of satellite base |

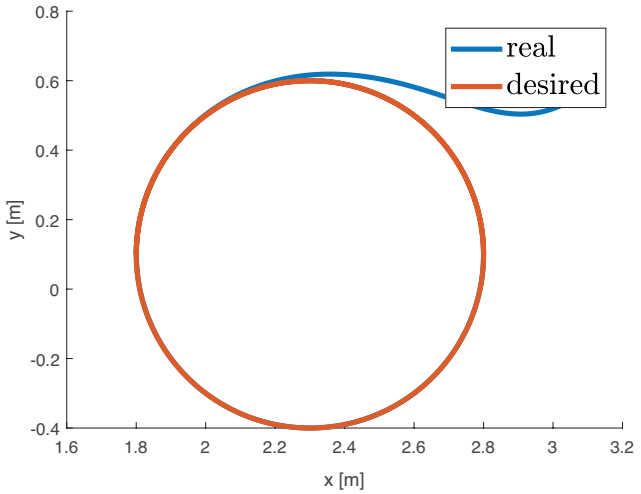


Fig. 2. Real and desired trajectory in XY plane tracked by end-effector

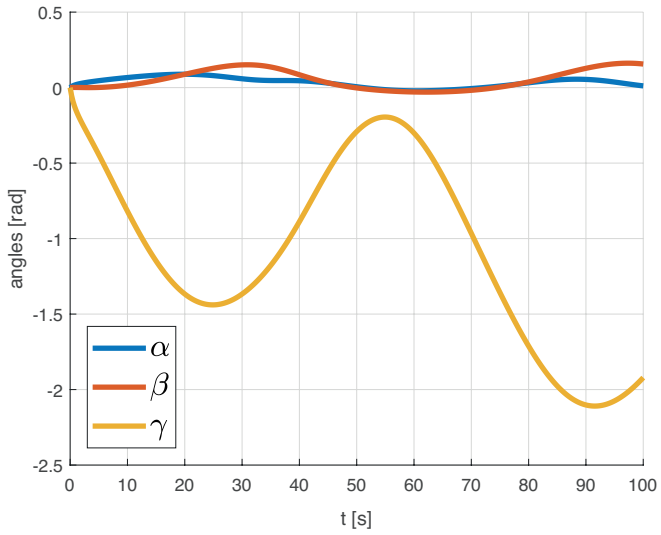


Fig. 3. Euler angles during trajectory tracking task

An example of the desired and real trajectory was presented in the Fig. 2 while the errors convergence for each scenario were presented in Figs 4–12.

In the Fig. 3 Euler angles for the satellite were presented during the trajectory tracking task.

**7.1. Noiseless control.** In the Fig. 4 error convergence for $e_x$, $e_y$ and $e_z$ was presented. This plot is a reference signal since during the simulation no additional noise was introduced.

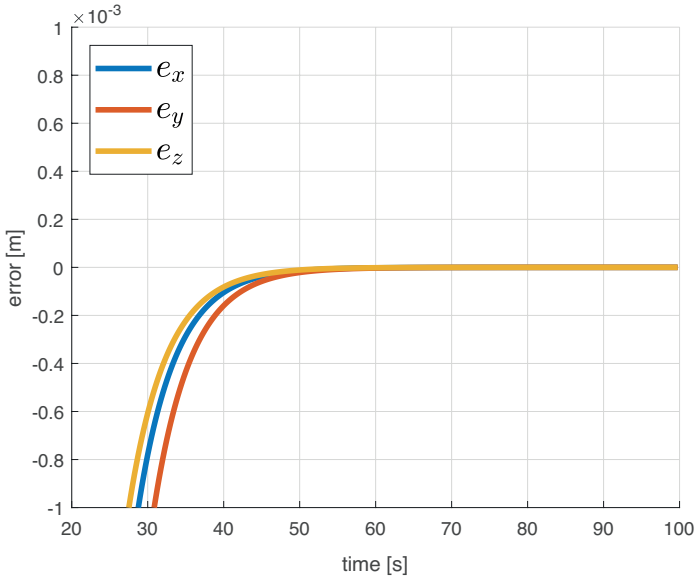


Fig. 4. Errors for scenario °0 (no noise)

**7.2. Noise in manipulator state and control.** Figures 5, 6 and 7 show error convergence for the class where small noise was added to the state vector (Fig. 5) and also noise to the control

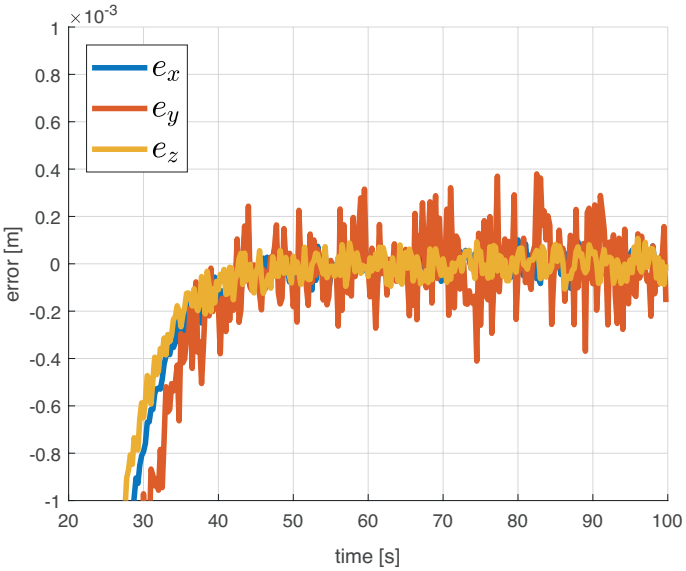


Fig. 5. Errors for scenario °1

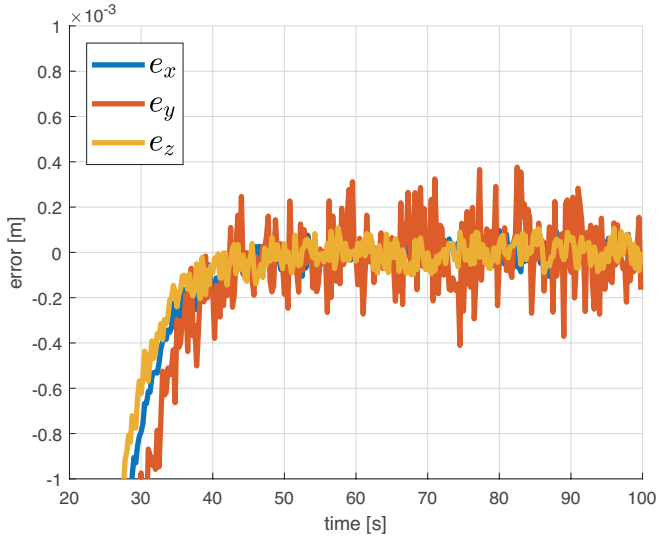


Fig. 6. Errors for scenario °2

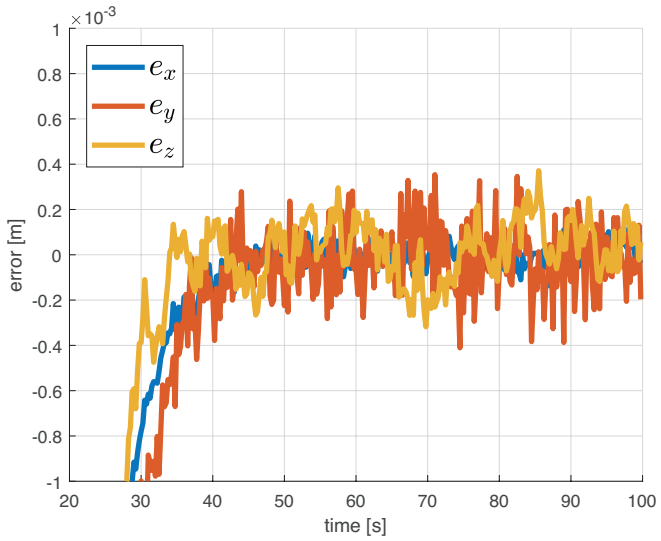


Fig. 7. Errors for scenario °3

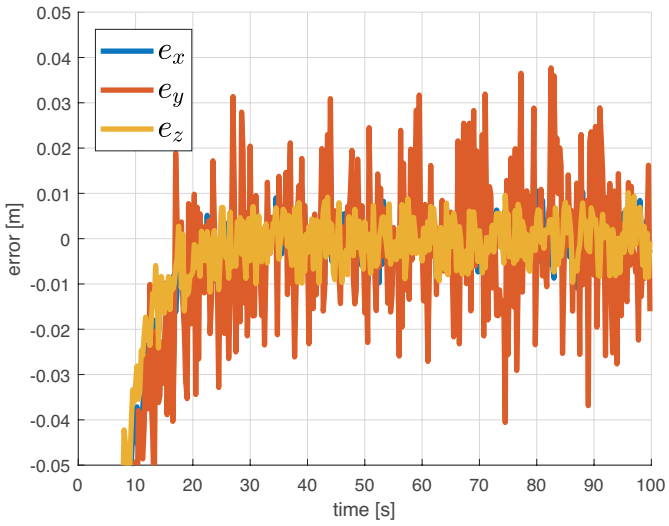


Fig. 8. Errors for scenario °4

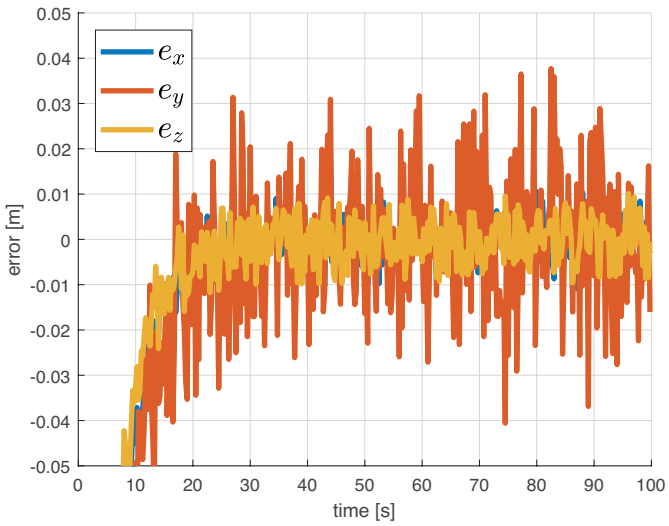


Fig. 9. Errors for scenario °5

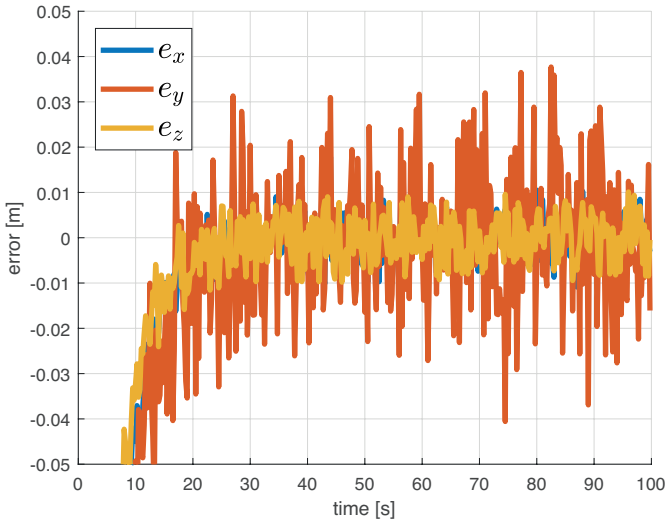


Fig. 10. Errors for scenario °6

input was introduced (Fig. 6 and Fig. 7). Those plots are very similar to each other which suggest that the increasing noise in control inputs has limited impact on the system.

However, when the disturbance to the state vector is increased by the order of two in its magnitude then it can be observed that this situation has significant effect on the system. Figs. 8, 9, and 10 present such situation. As previously the influence of control input noise was increased which still does not have a significant effect.

**7.3. Noise in control.** Considering plots which are classified as only noise disturbed control signals (Fig. 11 and Fig. 12) it can be seen that errors do not converge to zero, however, they are bounded. What is more, the magnitude of noise amplitude has a direct influence on control quality. The greater the noise of the amplitude the greater the errors present in the system.

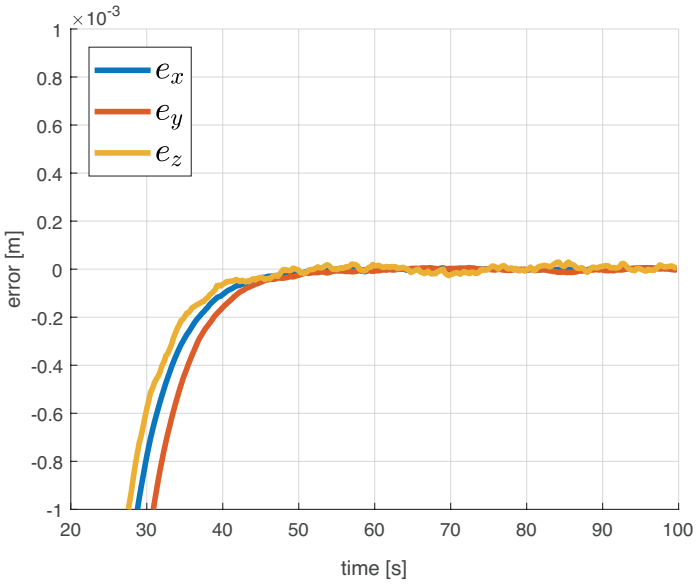


Fig. 11. Errors for scenario °7

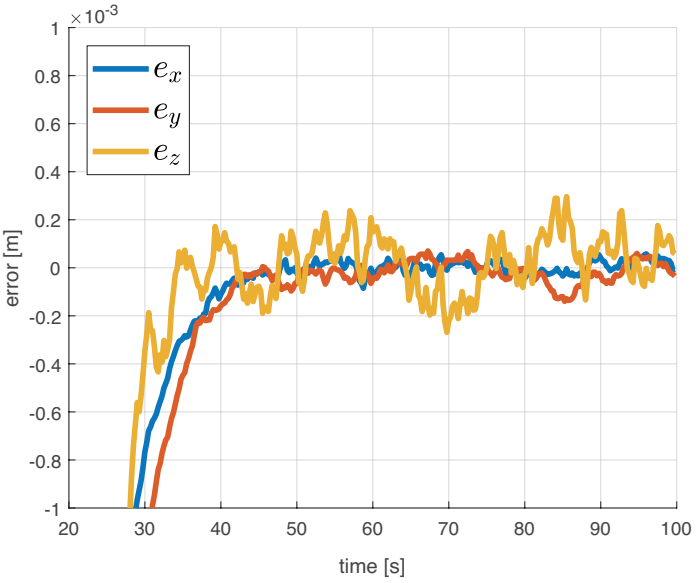


Fig. 12. Errors for scenario °8

## 8. Conclusions

During simulations it was confirmed that the proposed control algorithm, the input-output decoupling control, is working properly for the object, i.e. a satellite with a 3R manipulator. The desired trajectory was successfully recreated by the end–effector. A model with under-actuated dynamics was presented (21) where a matrix $G$ of rectangular shape was present. To derive a control algorithm for input–output decoupling approach it was shown that the matrix $G$ has a square and invertible $\bar{G}$ submatrix. $\bar{G}$ is of $3\times3$ size where it is directly used in control algorithm (35). In this work we have shown that proposed approach can be used for a situation where certain uncertainties are present in the system. We have derived four classes of noise disturbance depending on the part of the dynamics that is influenced. The first class describes an ideal case where there is no noise in the system. This situation is impossible to achieve in real system due to measurement errors, noise in actuators, etc. The most common practice to overcome those obstacles is to use a vision system [2, 21] or multisensor fusion [7]. However, it complicates the system. Adding noise to the manipulator state, angular position and velocity of its joints, and to control inputs was also investigated. Based on the simulation results it was shown that the algorithm works for the situation described above, but the most essential influence on the control quality has a noise in state variables, not in control signals.

**Acknowledgements.** The works of Wojciech Domski were supported by grant no. 0402/0107/18. The works of Alicja Mazur were supported by National Science Centre grant no. 2015/17/B/ST7/03995.

## References

[1] M.M.A. Al-Isawi and J.Z. Sasiadek, "Navigation and control of a space robot capturing moving target", In *2017 11th International Workshop on Robot Motion and Control (RoMoCo)*, 160–165, 2017.

[2] L. Changchun, Z. Xiaodong, P. Dong, and L. Xin, "Research of visual servo control system for space intelligent robot", In *2015 IEEE Advanced Information Technology, Electronic and Automation Control Conference (IAEAC)*, 96–100, 2015.

[3] W. Cheng, L. Tianxi, and Z. Yang, "Grasping strategy in space robot capturing floating target", *Chinese Journal of Aeronautics* 23(5), 591–598 (2010).

[4] W. Domski and A. Mazur, "Emergency control of a space 3R manipulator in case of one joint failure", In *22nd International Conference on Methods and Models in Automation & Robotics*, pages 384–389, 2017.

[5] N. Inaba, T. Nishimaki, M. Asano, and M. Oda, "Rescuing a stranded satellite in space – experimental study of satellite captures using a space manipulator", In *Proceedings 2003 IEEE/ RSJ International Conference on Intelligent Robots and Systems (IROS 2003) (Cat. No.03CH37453)* 4, 3071–3076 vol. 3, 2003.

[6] A. Isidori, *Nonlinear Control Systems*, Springer-Verlag London, 1995.

[7] R. Jassemi-Zargani and D. Necsulescu, "Extended kalman filterbased sensor fusion for operational space control of a robot arm", *IEEE Transactions on Instrumentation and Measurement* 51(6), 1279–1282, 2002.

[8] M. Kanazaki, Y. Yamada, and M. Nakamiya, "Trajectory optimization of a satellite for multiple active space debris removal based on a method for the traveling serviceman problem", In *2017 21st Asia Pacific Symposium on Intelligent and Evolutionary Systems (IES)*, 61–66, 2017.

[9] X. Li, Y. Yao, B. Yang, and L. Wang, "Guidance strategy design for space debris removal using fractionated spacecraft", In *2016 IEEE Chinese Guidance, Navigation and Control Conference (CGNCC)*, 264–270, 2016.

[10] A. Mazur and M. Cholewiński, "Implementation of factitious force method for control of 5R manipulator with skid-steering platform REX", *Bull. Pol. Ac.: Tech*. 64(1), 71–80 (2016).

[11] A. Mazur and B. Lukasik, "The input-output decoupling controller for nonholonomic mobile manipulators", In *Proceedings of the Fourth International Workshop on Robot Motion and Control (IEEE Cat. No.04EX891)*, 155–160, 2004.

[12] C. Meng, Z. Li, H. Sun, D. Yuan, X. Bai, and F. Zhou, "Satellite pose estimation via single perspective circle and line", *IEEE Transactions on Aerospace and Electronic Systems* 54(6), 3084–3095, Dec 2018.

[13] E. Papadopoulos and S. Dubowsky, "On the nature of control algorithms for free-floating space manipulators", In *IEEE Trans. on Robotics and Automation* 7, 750–758, 1991.

[14] R. Petrella, M. Tursini, L. Peretti, and M. Zigliotto, "Speed measurement algorithms for low-resolution incremental encoder equipped drives: a comparative analysis", In *2007 International Aegean Conference on Electrical Machines and Power Electronics*, pages 780–787, Sep. 2007.

[15] T. Rybus, "Obstacle avoidance in space robotics: Review of major challenges and proposed solutions", *Progress in Aerospace Sciences* 101, 31–48, August 2018.

[16] T. Rybus and K. Seweryn, "Application of rapidly-exploring random trees (RRT) algorithm for trajectory planning of freefloating space manipulator", In *2015 10th International Workshop on Robot Motion and Control (RoMoCo)*, 91–96, 2015.

[17] T. Rybus, K. Seweryn, and J. Z. Sasiadek, "Control system for free-floating space manipulator based on nonlinear model predictive control (NMPC)", *Journal of Intelligent & Robotic Systems* 85(3), 491–509, 2017.

[18] T. Rybus, K. Seweryn, and J. Z. Sasiadek. "Application of predictive control for manipulator mounted on a satellite", *Archives of Control Sciences* 28, 105–118, 2018.

[19] K. Seweryn, T. Rybus, P. Colmenarejo, G. Novelli, J. Oleś, M. Pietras, J.Z. Sasiadek, M. Scheper, and K. Tarenko, "Validation of the robot rendezvous and grasping manoeuvre using microgravity simulators", In *2018 IEEE International Conference on Robotics and Automation (ICRA)*, 873–880, 2018.

[20] B. Siciliano and O. Khatib, *Springer Handbook of Robotics*, Springer-Verlag New York, Inc., 2007.

[21] M.E. Stieber, M. McKay, G. Vukovich, and E. Petriu, "Vision based sensing and control for space robotics applications", *IEEE Transactions on Instrumentation and Measurement*, 48(4), 807–812, 1999.

[22] Y. Umetani and K. Yoshida, "Workspace and manipulability analysis of space manipulator", In *Trans. of the Society of Instrument and Control Engineers* E-1, 116–123 (2001).

[23] H. Wang, D. Guo, H. Xu, W. Chen, T. Liu, and K.K. Leang, "Eyein- hand tracking control of a free-floating space manipulator", *IEEE Transactions on Aerospace and Electronic Systems* 53(4), 1855–1865, 2017.